DEVELOPMENT OF TEMPERATURE STATISTICAL MODEL WHEN MACHINING OF AEROSPACE ALLOY MATERIALS

by

***Kumaran KADIRGAMA*[*1], *Mustafizur RAHMAN*[1], *Bashir MOHAMED*[2], *Rosli Abu BAKAR*[1], *and Ahmad Rasdan ISMAIL*[1]**

[1]Faculty of Mechanical Engineering, University Malaysia Pahang, Pahang, Malaysia
[2]Department of Mechanical Engineering, Faculty of Engineering, University Tenaga Nasional Bangi, Selangor, Malaysia

Original scientific paper
DOI: 10.2298/TSCI120203112K

This paper presents to develop first-order models for predicting the cutting temperature for end-milling operation of Hastelloy C-22HS by using four different coated carbide cutting tools and two different cutting environments. The first-order equations of cutting temperature are developed using the response surface methodology (RSM). The cutting variables are cutting speed, feed rate, and axial depth. The analyses are carried out with the aid of the statistical software package. It can be seen that the model is suitable to predict the longitudinal component of the cutting temperature close to those readings recorded experimentally with a 95% confident level. The results obtained from the predictive models are also compared with results obtained from finite-element analysis (FEA). The developed first-order equations for the cutting temperature revealed that the feed rate is the most crucial factor, followed by axial depth and cutting speed. The PVD coated cutting tools perform better than the CVD-coated cutting tools in terms of cutting temperature. The cutting tools coated with TiAlN perform better compared with other cutting tools during the machining performance of Hastelloy C-22HS. It followed by TiN/TiCN/TiN and CVD coated with TiN/TiCN/Al_2O_3 and TiN/TiCN/TiN. From the finite-element analysis, the distribution of the cutting temperature can be discussed. High temperature appears in the lower sliding friction zone and at the cutting tip of the cutting tool. Maximum temperature is developed at the rake face some distance away from the tool nose, however, before the chip lift away.

Key words*: Temperature, finite element analysis, PVD, Hastelloy C-22HS*

Introduction

Energy is concentrated in an extremely tiny zone during machining. The little fraction is stored in the workpiece and chip to increase the dislocation density. The vast majority of energy is converted into heat. Because the cutting zone keeps moving into the workpiece, there is little heating taking place ahead of the tool and, at least at high cutting speed condition, most of the heat (over 80 %) is carried away by the chip [1, 2]. However, the tool is in continuous contact with the chip and, in the absence of an effective heat-insulating

* Corresponding author, e- mail: kumaran@ump.edu.my

layer. The rake face of the tool is heated up. Rubbing on the rake face (or deformation in the secondary shear zone) is also a substantial source of heating. The maximum temperature is developed at the rake face located some distance away from the tool nose before the chip lifts away. As expected, both maximum (T_{max}) and average interface (T_{int}) temperatures increase with the increasing of cutting speed. The highest temperature that can be reached is the melting point of the material; hence, alloy in which its melting point is lower than the softening temperature of the tool (such as the Al and Mg alloys) can, in principle, be cut at any speed, especially with carbide tools [3]. Temperature can be estimated from dimensional analysis, assuming that all energy E is converted into heat [3]. The mean tool face temperature T_T can be expressed as eq. (1):

$$T_T = E\left(\frac{vh}{k\rho c}\right)^{1/2} \tag{1}$$

where k is the heat conductivity, ρ is the density, and c is the specific heat (heat content per unit volume) of the workpiece material, v is the cutting speed and h is the height.

Thus, higher temperature is expected when cutting stronger materials (higher E) at higher-speed condition, especially if the workpiece material is a poor heat conductor, with low density and low specific heat. Materials such as titanium and superalloys are difficult to machine, in contrast with aluminum and magnesium. Even though most of the heat is taken away by the chip, some portions diffuse into the workpiece. The resulting dimensional change must be compensated for, and heat buildup in the tool is a significant factor limiting the cutting speed [3]. Usui and Shirakachi [4] assumed the shear cutting angle, chip geometry and flow line in order to predict parameters such as stress, strain and temperature. Tieu et al. [5] included the effect of adhering layer formation on the tool into the finite-element analysis. The temperature gradient vertical to the rake face is smaller as compared to that of the adhering layer. Ng et al. [6] employed the finite-element method to calculate the cutting force and temperature distribution. They have used the experimental data obtained from the infrared and cutting force measurements in order to validate their model. At lower heat conductance, the amount of heat carried by the chip and the temperature of the tool–chip interface is higher. Deformation of work material, contact property, friction, large plastic strain, strain-hardening, and thermal softening play a vital role in chip formation mechanism. Simulations for optimum design of machine tools and tool geometry have been carried out to provide some practical solutions to improve the process output. The aim of this paper is to develop the statistical model to predict the temperature for end-milling operation of Hastelloy C-22HS with different coated carbide cutting tools and different cutting environments.

Finite Element Analysis

Third Wave AdvantEdge from Minneapolis is a special program written for machining simulations. It is developed based on the dynamic explicit Lagrangian formulation. The model is built by selecting the type of machining operation (e.g. turning, broaching, sawing or milling) and defining the necessary process parameters. Since the main subject of this work is related to milling operation, the process parameters are feed rate, axial depth of cut, length of cut, radial depth, spindle speed and initial temperature of the workpiece. The model created by Third Wave AdvantEdge is also thermo-mechanically coupled. In Third Wave AdvantEdge, a staggered procedure is adopted for the purpose of coupling the thermal and mechanical equations [7]. Geometrically identical meshes for the thermal and mechanical

models are used. Mechanical and thermal computations are staggered, assuming the constant temperature during the mechanical step and constant heat generation during the thermal step. A mechanical step is taken first based on the current distribution of temperature, and the heat generated is computed from plastic working and frictional heat generation.

The heat thus computed is transferred to the thermal mesh and the temperatures are recomputed by recourse to the forward-Euler algorithm. The resulting temperatures are transferred to the mechanical mesh and incorporated into the thermal-softening model, which completes one time-stepping cycle. Thermal boundary conditions for Third Wave AdvantEdge are given as follows:

1. The heat is generated due to heavy plastic work done on the workpiece. It is computed as eq. (2) [7]:

$$R = \frac{m \cdot f \cdot W^P}{\rho} \tag{2}$$

where, W^P is the rate of plastic work, f is the fraction of plastic work converted into heat, m is the mechanical equivalent of heat and ρ is the density of workpiece material

2. The heat is generated due to friction between the chip and the rake face of the tool, which is expressed as eq. (3):

$$q = F_{fr} \cdot V_r \cdot m \tag{3}$$

where F_{fr} is the friction force, V_r is the relative sliding velocity between tool and chip and m is the mechanical equivalent of heat.

3. The generated frictional heat is distributed to chip and tool according to eq. (4) [7]:

$$\frac{Q_{chip}}{Q_{tool}} = \frac{\sqrt{k_{chip} \times \rho_{chip} \times c_{chip}}}{\sqrt{k_{tool} \times \rho_{tool} \times c_{tool}}} \tag{4}$$

where Q_{chip} is the heat given to the chip, Q_{tool} is the heat given to the tool, k is the conductivity, ρ is the density and c is the heat capacity.

Certain assumptions are made to simulate the complex procedure of metal cutting with FEM as listed below. These assumptions are used to define the problem to be solved as well as to apply the boundary and loading conditions:

i) The cutting speed is constant.
ii) The width of cut is larger than the feed (plane strain condition), and both are constant.
iii) The cutting velocity vector is normal to the cutting edge.
iv) The workpiece material is a homogeneous polycrystalline, isotropic, and incompressible solid.
v) The workpiece is set at a reference temperature of 20° C at the beginning of the simulation.
vi) The machine tool is perfectly rigid and no influence of machine tool dynamics on machining is considered.
vii) The friction is constant at tool-chip interaction and tool-workpiece interaction.

The finite deformation formulation used in Third Wave AdvantEdge incorporates the six-noded quadratic triangular elements for spatial discretization. The element has three corners and three mid-side nodes, providing quadratic interpolation of the displacement within the element [8]. The separation of nodes, thus forming the chip from the workpiece during a cutting simulation, is achieved by continuous remeshing. Therefore, during the metal-cutting process, the workpiece material is allowed to flow around the cutting tool edge and when the elements in the vicinity become distorted, Third Wave Advant Edge updates finite element mesh periodically by refining large elements, remeshing distorted elements, and coarsening small elements. The initial positions of the workpiece and cutting tool with selected mesh setting are shown in fig. 1.

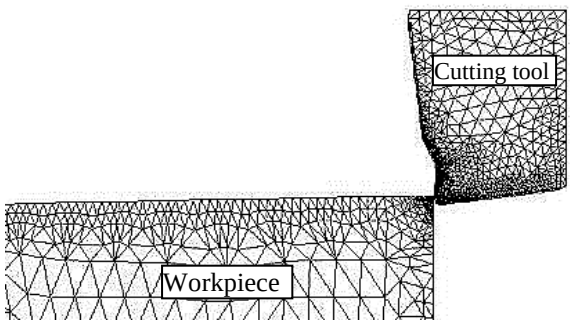

Figure 1. The initial position of the workpiece and cutting tool with selected mesh.

As it has been mentioned before in a typical machining event, extremely high strain rates, in excess of 10^4 s^{-1} may be attained within the primary and secondary shear zones, while the remainder of the workpiece deforms at moderate or low strain rates. In order to account for a variation in the strain rate sensitivity at low and high strain rates, Third Wave AdvantEdge incorporates a stepwise variation of the rate sensitivity exponent *m* while maintaining continuity of stress. This leads to the following relations for low and high strain-rates [9].

$$\bar{\sigma} = \sigma_f\left(\varepsilon^p\right)\cdot\left(1+\frac{\dot{\varepsilon}^p}{\dot{\varepsilon}_o^p}\right)^{1/m_2}\cdot\left(1+\frac{\dot{\varepsilon}_t}{\dot{\varepsilon}_o^p}\right)^{1/m_1} \tag{5}$$

where $\bar{\sigma}$ is the effective von Mises stress, σ_f is the flow stress, ε^p is the accumulated plastic strain, $\dot{\varepsilon}_o^p$ is a reference plastic strain rate, m_1 and m_2 are low and high strain-rate sensitivity exponents, respectively, and $\dot{\varepsilon}_t$ is the threshold strain rate which separates the two regimes. For calculations, a local Newton – Raphson iteration is used to compute $\dot{\varepsilon}_o^p$ according to the low – rate equation, and the high rate equation is used if the result lies above $\dot{\varepsilon}_t$. σ_f , which is used in Eq. (4), can be expressed as eq. (5) [9]:

$$\sigma_f = \sigma_0\cdot\psi(T)\cdot\left(1+\frac{\varepsilon^p}{\varepsilon_0^p}\right)^{1/n} \tag{6}$$

where T is the current temperature, σ_0 is the initial yield stress at the reference temperature T_0, ε_0^p, is the reference plastic strain, n is the hardening exponent $\varepsilon^p$is the accumulated plastic strain and $\Psi(T)$ is the thermal softening factor. In the present study, it is assumed that the tool material is not effected by plastic deformation. Hence, it is considered as fully rigid. Heat can be transferred to the tool only from the workpiece. The initial coolant temperature is selected as the room temperature. Heat flux due to coolant is applied to all exposed and non-contacting surfaces on the tool and workpiece, except the bottom face of the workpiece and the faces on the tool where constant temperature is applied.

Experimental set-up

The tool inserts are made by Kennametal on the basis of the ISO catalogue number of SPHX1205ZCFRGN1W (KC725M, KC520M, KC915M and KC930M). KC520M is a coated carbide grade with TiAlN coating PVD. TiAlN is a hard, abrasion-resistant coating with high temperature resistance developed specially for high speed and dry machining applications. KC725M is a coated carbide grade with TiN/TiCN/TiN coating PVD. The excellent thermal shock resistance of the substrate makes this grade ideal for wet and dry machining. KC915M is a coated carbide grade with CVD multilayer coating TiN/TiCN/Al_2O_3. KC915M can be used in wet and dry machining. KC930M is a coated carbide grade with CVD multilayer coating TiN/TiCN/TiN. It can be used both in dry and wet machining. Coated carbide tool bits are made by depositing an extremely thin layer of wear resistant material such as titanium nitride, titanium carbide or aluminum oxide on the cutting edge of the cutting tool. This layer decreases friction, improves the wear resistance of cutting edge by 200-500% and enhances the breakage resistance of the tool while providing longer life and increased cutting speeds [10]. The overall coating thickness is 3 to 3.5 μm. Flood coolant was used in this study. In this study, only one insert per one experiment is mounted on the cutter. The cutting tools implemented in this experiment are shown fig. 2. The following is the details of the tool geometry square end mills inserts when mounted in the tool holder: a) Square shape

b) Axial Rake angle: 6°
c) End relief angle: 5°
d) Sharp cutting edge

Table 1. Composition of the cutting tool

Code name	Composition (%)						Coating	Thickness (μm)
	% Co	% WC	%Cr3C2	%TaC	%TiC	%Nbc		
KC915M	10.5	72	-	7	7	3.5	CVD TiN/TiCN/Al_2O_3	3
KC725M	11.5	88	0.5	-	-	-	PVD TiN/TiCN/TiN	3
KC520M	6	93.5	0.5	-	-	-	PVD TiAlN	3.5
KC930M	6	91.5	0.5	-	-	-	CVD TiN/TiCN/TiN	3

Square-shaped inserts give longer tool life as well as the better surface finish [11]. This is due to the increase of included angles of round and square inserts, which tends to

increase the edge strength of the inserts and tool–chip contact area, resulting in lower stress and temperature level at the cutting edge. Manjunathaiah and Endres [12] have investigated the effect of nose radius on tool flank wear. They have reported that for sharp tools, there exists the nose radius that minimizes the tool flank wear both at the lead edge and at the tool tip. The composition of the cutting tool is shown in tab. 1. The insert was mounted on 90 degree (50A04RP90SP12CFP) tool holder.

The suitable levels of the factors are used to deduce the design parameters for Hastelloy C-22HS, which is shown in tab. 2. The lower and higher-speed values were selected of 100 m/min and 180 m/min, respectively. The ranges of feed rate, axial depth are 0.1 to 0.2 mm per tooth and 1 to 2 mm respectively. Radial depth of 3.5 mm is selected for all experiments.

Table 2. The values selected for the variables

Factors/Coding of Levels	-1	0	1
Speed, V_c (m/min)	100	140	180
Feed, f (mm/tooth)	0.1	0.15	0.2
Axial depth, a_d(mm)	1	1.5	2

Hastelloy C-22HS nickel based alloy blocks supplied by Haynes International were used for the experiments. The blocks were in annealed condition where its hardness around Rockwell B 90. Each block was prepared 180 mm long, 100 mm wide and 20 mm high was used in the trials. The physical properties of the workpiece material (Hastelloy C-22HS) are shown in tab. 3 [13]. The machine center is driven by a 7.5 kW electric motor which provides high torque. A vertical machine center OKUMA MX45-VA was used for all operations that preparing the workpiece or cutoff were required. Experimental setup is shown in fig. 2.

Table 3. Physical properties of Hastelloy C-22HS at room temperature

Properties	Value
Density (g/cm^3)	8.6
Thermal Conductivity (W/m.^{o}C)	11.8
Mean Coefficient of Thermal Expansion (μm/m.^{o}C)	11.6
Thermal Diffusivity (cm^2/s)	0.0334
Specific Heat (J/kg.^{o}C)	412
Young Modulus (GPa)	223

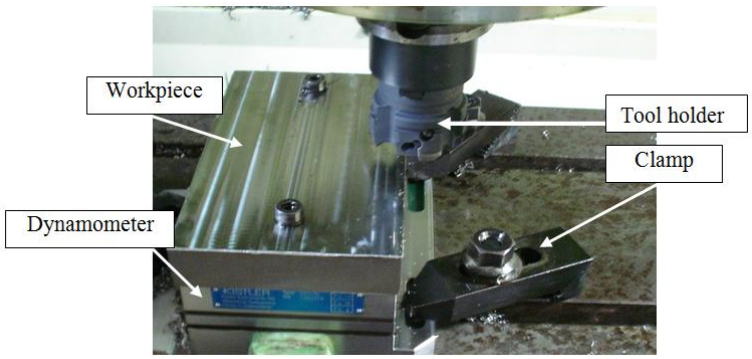

Figure 2. Experimental set-up

Results and Discussion

After conducting the first pass (one pass is equal to 90 mm length) of the 15 cutting experiments, the cutting temperature readings are used to find the parameters appearing in the postulated first-order model. In order to determine these parameters, the least square method is used with the aid of statistical software. The first-order linear equation for predicting the cutting temperatures can be expressed as eq. (7-10):

(KC520M) $$Temperature = 161.03 + 0.56x_1 + 144.5x_2 + 10.08x_3 \quad (7)$$

(KC725M) $$Temperature = 85.80 + 0.90x_1 + 275x_2 + 30.75x_3 \quad (8)$$

(KC915M) $$Temperature = 164.68 + 0.84x_1 + 92.5x_2 + 16.75x_3 \quad (9)$$

(KC930M) $$Temperature = 88.76 + 1.13x_1 + 365x_2 + 35.25x_3 \quad (10)$$

From this linear eq. (7-10), one can easily notice that the cutting temperature is affected significantly by the feed rate followed by the axial depth of cut and the cutting speed, for all models. Generally, the increase in feed rate, axial depths and cutting speed will cause the cutting temperature to increase [14]. Increasing either the radial or axial depth of cut increases the workpiece temperature, while use of cutting fluid dramatically reduces the workpiece temperature [15]. The results obtained agree with Kitagawa et al. [16] where the temperature rises monotonically with increasing cutting speed when machining Inconel 718. Fig. 3 shows the cutting temperature at high cutting speed (180 m/min) meanwhile fig. 4 shows the cutting temperature at low cutting speed (100 m/min). The cutting temperatures increased gradually when increase the cutting speed and feed rate. It can be seen in fig. 3 where the temperature for four cutting tools increased gradually from experiment 1 to experiment 3 as the increase the feed rate from 0.1 mm/tooth to 0.2 mm/tooth. These findings are in agreement with the previous studies [17]. Same observation made by Korkut [18] where increase the cutting speed it directly increases the cutting temperature by 3 ~10 %. This situation indicates that the energy required for the plastic deformation of the workpiece reaches a sufficient level at the higher cutting. Therefore, the required energy for the further plastic deformation decreases with the further increase in the cutting speed and the heat developed in the deformation zone decreases. It observed that increased in axial depth contributed in temperature rising as can be seen in fig. 3 where the temperature increases from Experiment 1 to Experiment 2 when the increase axial depth from 1 mm to 2 mm. The temperature drops for the entire cutting tool when axial depth reduces from 2 mm to 1 mm. This observation also observed by Korkut [18] when increase the depth of cut the temperature increase gradually. According to this study, the phenomenon occur due to conversion of the increasing mechanical energy to the heat energy as the energy required for the plastic deformation of the workpiece does not reach an adequate level. At low cutting speeds, the shear speed and the chip speed also decrease. This situation increases the contact time of the chip when it moves on the rake face of the cutting tool. This, in turn, increases the temperature in the cutting zone. The temperature measured is not same with the temperature values observed by other researchers when machining nickel based superalloy [19]. This is because they used a different method to measure cutting temperature. However, the objective

of the temperature measurement study is to determine the changing temperature for different cutting parameters. Lee et al. [20] have also reported that the nickel-based alloy, which is high in strength, causes high temperature and stress at the tool–chip contact area. Although nickel-based alloys are not exceptionally hard but their outstanding high temperature strength and extreme toughness create difficulties during machining due to their tendencies of work hardening which result in particularly high cutting forces during machining [21].

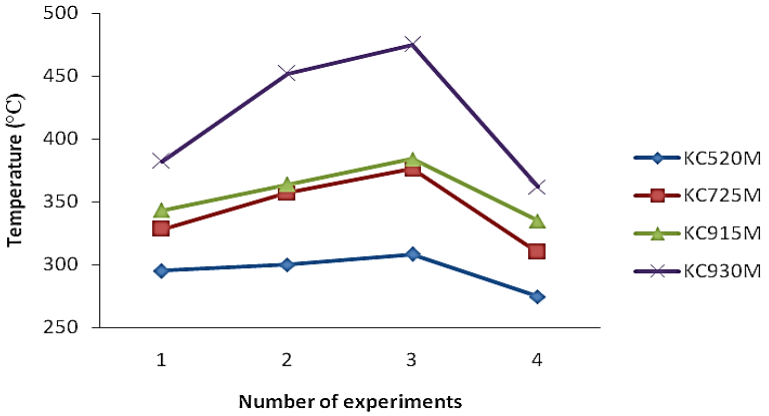

Figure 3. Selection 4 experiments from 15 experiments, combination of high cutting speed, feed rate and axial depth with coolant.

Experiment 1, cutting speed = 180 m/min, feed rate = 0.1 mm/tooth, axial depth = 1.5 mm
Experiment 2, cutting speed = 180 m/min, feed rate = 0.15 mm/tooth, axial depth = 2 mm
Experiment 3, cutting speed = 180 m/min, feed rate = 0.2 mm/tooth, axial depth = 1.5 mm
Experiment 4, cutting speed = 180 m/min, feed rate = 0.15 mm/tooth, axial depth = 1 mm

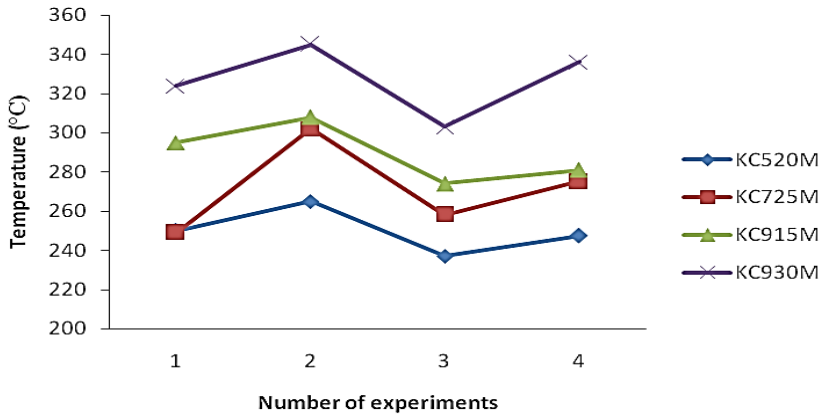

Figure 4. Selection 4 experiments from 15 experiments, combination of low cutting speed, feed rate and axial depth with coolant.

Experiment 1, cutting speed = 100 m/min, feed rate = 0.15 mm/tooth, axial depth = 1 mm
Experiment 2, cutting speed = 100 m/min, feed rate = 0.15 mm/tooth, axial depth = 2 mm
Experiment 3, cutting speed = 100 m/min, feed rate = 0.1 mm/tooth, axial depth = 1.5 mm
Experiment 4, cutting speed = 100 m/min, feed rate = 0.2 mm/tooth, axial depth = 1.5 mm

The temperature of four inserts increases with dry cutting as shown in fig. 5. This can be explained that coolant is one of the most influential factors affecting the tool performance when machining nickel-based alloys [22- 23]. The longer tool life achieved when machining was alloy with sialon ceramic tool is attributed to the reduction of the overall temperature in the cutting area. The glassy phase (b prime grains) in the sialon tool matrix will start to soften at 1000 °C.The The application of coolant will retard the removal of the b-prime grains by preventing its softening process. The improved performance observed when machining Incoloy 901 and Inconel 718 with SiC whisker-reinforced alumna ceramic tool may be also attributed to the lower temperature developed, which tends to reduce the thermal stresses arising from the differential expansion between the silicon carbide and alumina [23]. In the present work, the PVD cutting tools generated lower temperatures compare with CVD cutting tools. The main difference between PVD and CVD is the former's relatively low processing temperature -500ºC [24]. This lower processing temperature result in multiple benefits for PVD coatings such as the grain structure of the coating is remarkably fine. The result is a remarkably smooth, bright coating with a low coefficient of friction. PVD coatings are essentially free of the thermal cracks that are common in CVD coatings [24]. TiAlN coated cutting tool produced low temperature compares to other coated cutting tools. The key to TiAlN's performance is the addition of aluminum, which may oxidize during machining to form an extremely thin layer of Al_2O_3 [25]. Higher aluminum: titanium ratios 2: 1, versus 1.5: 1 in a typical TiAlN coating--result in improved resistance to chattering and better high-speed capability in titanium and exotic alloys [24]. TiN/TiCN/Al_2O_3 CVD produces low tempe-rature compare with CVD TiN/TiCN/TiN since Al_2O_3 provides excellent thermal heating and oxidation resistances as well as abrasive wear as shown in fig. 6.

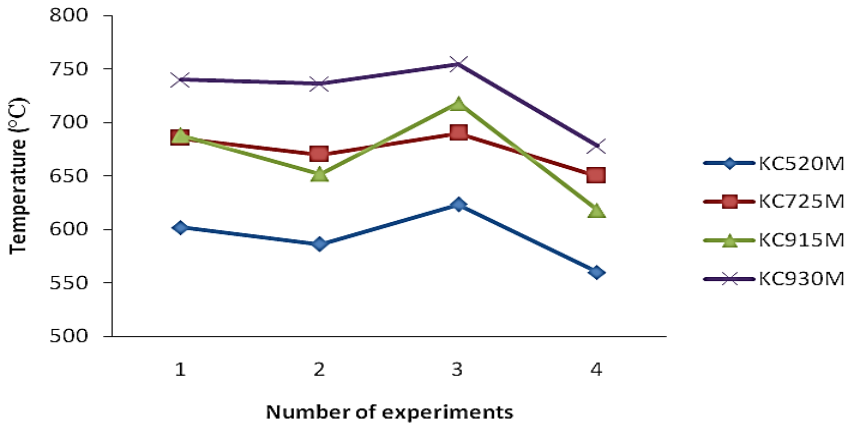

Figure 5. Selection 4 experiments from 15 experiments, combination of low cutting speed, feed rate and axial depth without coolant.

Experiment 1, cutting speed = 180 m/min, feed rate = 0.1 mm/tooth, axial depth = 1.5 mm
Experiment 2, cutting speed = 180 m/min, feed rate = 0.15 mm/tooth, axial depth = 2 mm
Experiment 3, cutting speed = 180 m/min, feed rate = 0.2 mm/tooth, axial depth = 1.5 mm
Experiment 4, cutting speed = 180 m/min, feed rate = 0.15 mm/tooth, axial depth = 1 mm

When metal is cut, the material is deformed plastically, and the energy is expanded in deforming the chip and in overcoming friction between the tool and workpiece. Almost all of the energy is converted into heat [23]. The heat is mainly generated in two regions: the shear zone (primary deformation zone), and the rake face zone which is the zone in the tool/work interface (the secondary deformation zone). In addition, some heat may generate in the tool clearance face/work surface zone due to friction when the cutting tool is not perfectly sharp. High temperature on the rake face of the tool may soften and wear the tool, and have a strong influence on tool life [23]. Furthermore, the temperature activated tool wear mechanism limits the material removal rate. Finally, the heat generated at the tool clearance face affects the finish and metallurgical state of the machined surface. Heat entering the workpiece influences the dimension accuracy and surface quality of the machined part. While much of the heat generated in the three zones mainly passes to the tool, workpiece and chip. Some fraction also lost to the surrounding air or the cutting fluid via convection [23].

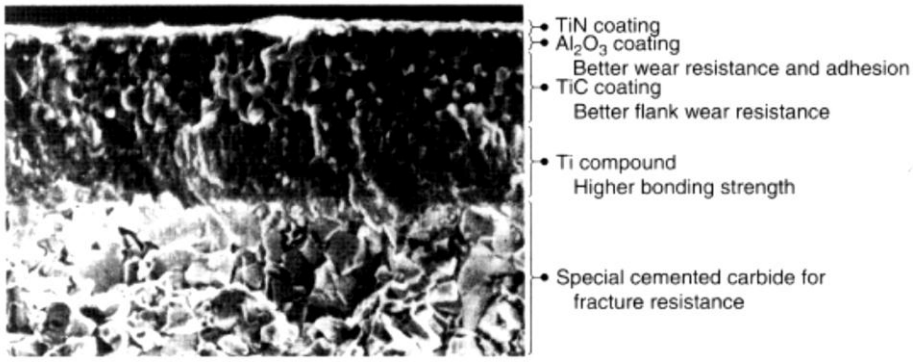

Figure 6. Schematic of multilayer coating [8]

Figure 7 shows the measured cutting temperature values and those predicted by the first-order model. It is clear that the predicted values agree well with the experimental readings. This indicates that the obtained linear model is useful to predict the cutting temperature. The adequacy of the first-order model is verified using the ANOVA. At a level of confidence of 95%, the model is checked for its adequacy. As shown in tab. 4, the P value is not significant with the lack-of fit (< 0.05). This implies that the model could fit, and it is adequate [25-26]. Contour plots are shown in fig. 8. The ANOVA results and contour plot for other cutting tools are not shown since TIAL coated cutting tool perform better than other cutting tools.

Table 4. Variance analysis for first order cutting temperature model – KC520M

Source	Degree of freedom	F-static	P-value
Regression	3	12.98	0
Linear	3	12.98	0
Residual Error	11		
Lack-of-Fit	9	3.03	0.273
Pure Error	2		
Total	14		

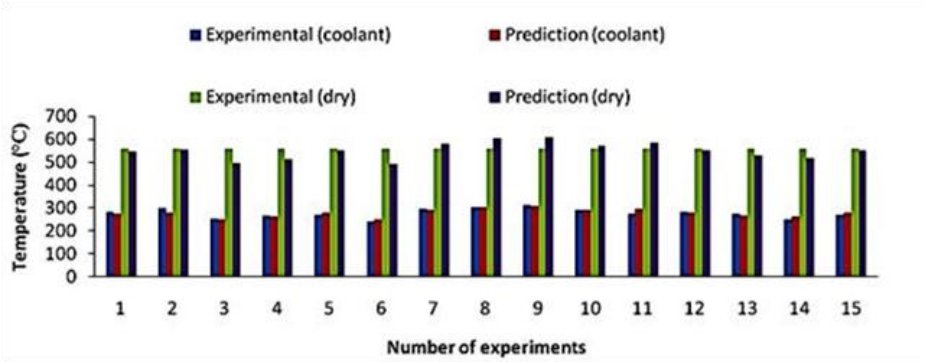

Figures 7. The comparison between the measured cutting temperature and predicted by the first-order model.

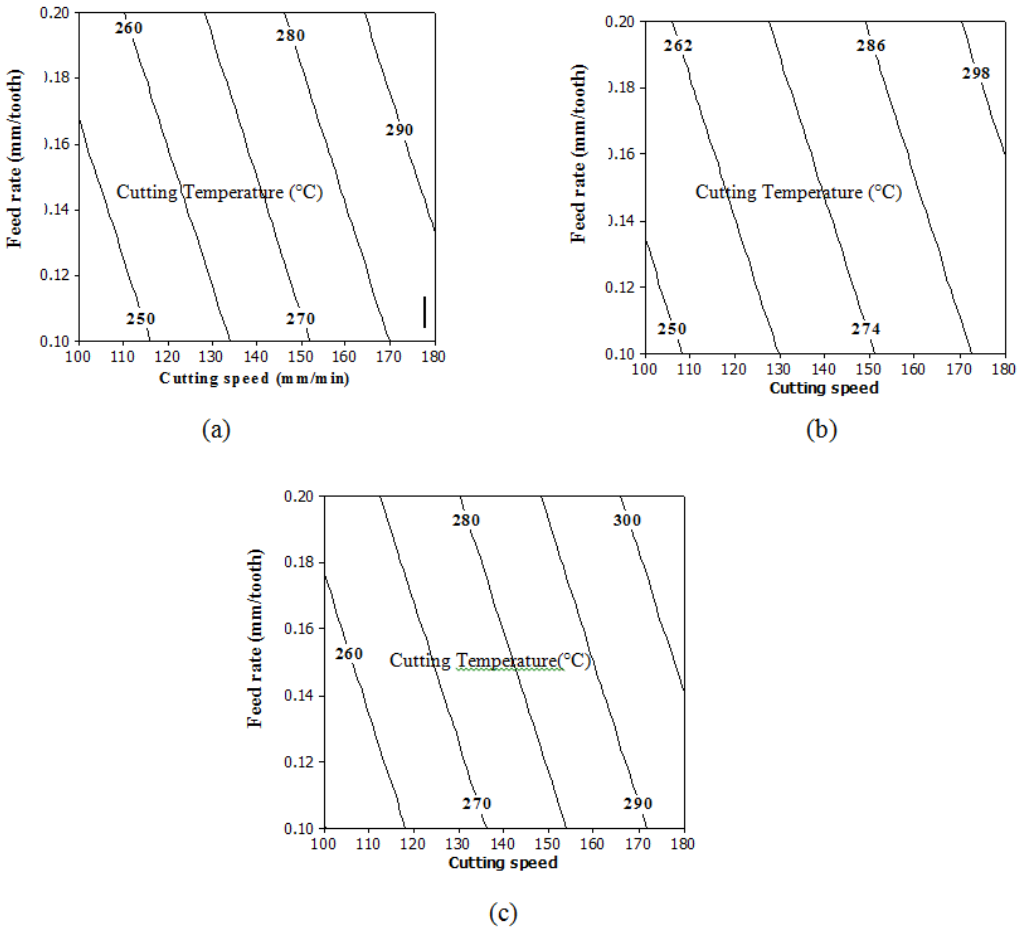

Figure 8. Cutting temperature contours in the cutting speed-feed rate plane for (a) axial depth 1 mm, (b) axial depth 1.5 mm, (c) axial depth 2 mm – KC520M.

Figure 9 (a) shows the temperature distribution obtained from the 3D simulation of the cutting tool. As seen, high-temperature region occurs at the cutting tool tip and in the rake face. According to Tay et al. [27], maximum temperature is developed at the rake face, located some distance away from the tool nose but before where the chip lifts away. Similar trends have been presented in [28-29]. Fig. 9(b) shows the comparison between predicted and experimental values. The predicted values are not very close (% difference = 20 to 25) to the experimental values, even though its accuracy is slightly inferior as compared to RSM. However, FEA can produce the temperature distribution around the cutting tool, in great detail. The predicted values deviate slightly from the experimental values due to the employed friction value [30]. However, the use of FEM in metal-cutting research requires a large number of input parameters, which need to be determined through an extensive experimental work and mechanical property tests. These include material models for large deformation, high strain rate, temperature effects, tool-chip contact and friction models, and the separation criterion [31].

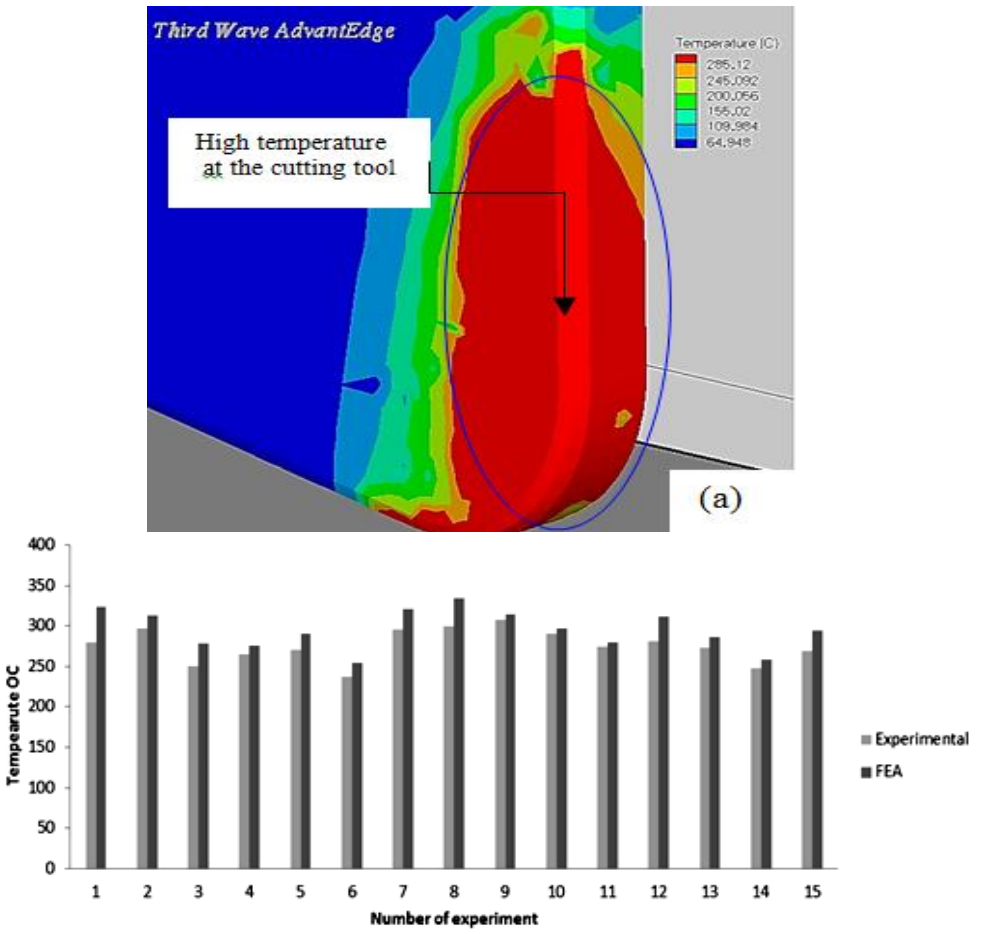

Figure 9. (a) 3D simulation for the cutting tool; (b) Prediction cutting temperature by FEA and experimental data – KC520M.

Conclusion

In the present research, first and second order mathematic models were developed to predict cutting parameters for Hastelloy C-22HS using four different coated carbide cutting tools and two different cutting environments. Finite element method used to find the distribution of the cutting temperature. It can be concluded from the result and discussion as follows:

a) The cutting temperature is affected significantly by the feed rate followed by the axial depth of cut and the cutting speed, for all models. Generally, the increase in feed rate, axial depths and cutting speed will cause the cutting temperature to increase.
b) From the finite-element analysis, the distribution of the cutting temperature can be discussed. High temperature appears in the lower sliding friction region and at the cutting tip of the cutting tool. Maximum temperature is developed at the rake face some distance away from the tool nose but before the chip lift away.
c) The PVD coated cutting tools perform better than the CVD coated cutting tools in terms of cutting temperature when machining Hastelloy C-22HS. The cutting tools coated with TiAlN perform to better compare with other cutting tools when machining Hastelloy C-22HS with current parameters. It followed by TiN/TiCN/TiN and CVD coated with TiN/TiCN/Al_2O_3 and TiN/TiCN/TiN.

Acknowledgment

The financial support by Malaysian Government through MOSTI, University Tenaga Nasional and University Malaysia Pahang is grateful acknowledged.

References

[1] Matsumoto, Y., Barash, M.M., Liu, C.R., Effect of hardness on the surface integrity of AISI 4340 steel, *J. Eng. Ind. Trans. ASME*, 108 (1986), 3, pp. 169–175.
[2] Dewes, R.C., Ng, E.G., Chua, C.K., Newton, P.G., Aspinwall, D.K., Temperature measurement when high speed machining hardened mould/die steel, *J. Mater. Process. Technol.*, 92 (1999), 93, pp. 293–301.
[3] Astakhov, V.P., Metal cutting mechanics, CRC press, 1999, Boka Raton, FL, USA
[4] Usui, K. , Shirakashi, T., Mechanics of machining from descriptive to predictive theory, on the art of cutting metals, *ASME PED*, 7 (1982), 1, pp. 13 -35
[5] Tieu, A.K., Fang, X.D., Zhang, D., FE analysis of cutting tool temperature field with adhering layer formation, *Wear*, 214 (1982), 2, pp. 252-258.
[6] Ng, E.G., Aspinwall, D.K., Brazil, D., Monaghan, J., Modelling of temperature and forces when orthogonally machining hardened steel, *Int. J. Mach. Tools Manuf.*, 39 (1999), 6, pp. 885–993.
[7] Soo, S., Aspinwall, D., Dewes, R., 3D FE modelling of the cutting of Inconel 718, *J. Mater. Process. Technol.*, 150 (2004), pp. 116-123.
[8] Marusich, T. D., Effects of friction and cutting speed on cutting force, *ASME MED23313*, (2001), 1-2, pp. 115-123.
[9] Marusich, T. D., Ortiz, M., Modeling and simulation of high-speed machining, *Int. J. Num. Meth. Eng*., 38 (1995), 1, pp. 75-94.
[10] Stimimann, J., Kirchheim, A., New Cutting force Dynamometer for high precision machining, *Industrial Tooling Conf.*, Sauthempton, UK, (1997), pp. 1-7.
[11] Ezugwu, E.O., Pashby, I.R., High speed milling of nickel-based superalloys, *J. Mater. Process. Technol.*, 3 (1992), pp.429–437.
[12] Manjunathaiah, J., Endres, J.W., A new model and analysis of orthogonal machining with an edge-radius tool, *Trans.ASME, J. Manufac. Sci.Eng.*, 122 (2000), pp. 384-390.

[13] Kennalmetal metal cutting catalogue (2007).
[14] Kadirgama, K., Abou-El-Hossein, K.A., Mohammad, B., Habeeb, H., Numerical and statistical model to determine temperature and heat distribution when machining HASTELLOY C-22HS, *Inter. Bull. Stat. Eco.*, 1 (2007), pp. 24-41.
[15] Shen, G. Modelling the effect of cutting fluids in peripheral milling, PhD thesis (1996)
[16] Kitagawa, T., Kubo, A., Maekawa, K., Temperature and wear of cutting tools in high speed machining of Inconel 718 and Ti -6Al-6V-2Sn, *Wear*, 202 (1997), 2, pp.142-148.
[17] Shaw, M.C., Metal cutting principles, Oxford University Press, New York, USA (1986).
[18] Korkut, I., Boy, M., Karacan, I., Seker, U., Investigation of chip-back temperature during machining depending on cutting parameters, *Mater. Des.*, 28 (2007), pp. 2329–2335.
[19] Muraka, P.D., Barrow, G., Hinduja, S., Influence of the process variables on the temperature distribution in orthogonal machining using the finite element method, *Int. J. Mech. Sci.*, 21 (1979), 8, pp. 445–456.
[20] Lee, M., Horne, J.G., Tabor, D., 1979, The mechanism of notch formation at depth of cut line of ceramic tools machining nickel-base superalloys, *Proc. 2nd Int. Conf., Wear Materials*, Dearborn, MI, USA, (1979), pp. 460–464.
[21] Warburton, P., Problems of machining nickel-based alloys, Iron and Steel Institute, *Special Report*, 94 (1967), pp. 151–160.
[22] Ezugwu, E.O., Machado, A.R., Pashby, I.R., Wallbank, J., The effect of high-pressure coolant supply when Machining a Heat-Resistant Nickel-Based Superalloy, Lub. Eng., 47 (1990), 9, pp.751-757.
[23] Pfouts, W. R. 2000, Cutting edge coatings, *Manufac. Eng.*, 125, (2000), 1, pp. 98-107.
[24] Destefani, J., Cutting tools 101: coatings, *Manufac. Eng.*, October 2002.
[25] Kadirgama, K., Abou-El-Hossein, K.A., Force prediction model for milling 618 tool steel using response surface methodology, *Am. J. Appl. Sci.*, 8 (2005), pp. 1222-1227.
[26] Kadirgama, K., Abou-El-Hossein, K.A. Torque and cutting force prediction model by using response surface method, *Int. J. Appl. Math. Stat.*, 4 (2006), MO5, pp. 11-30.
[27] Tay, A.O., Stevenson, M.G., de Vahl Davis, G., Oxley, P.L.B., Using the finite element method to determine temperature distributions in orthogonal machining, *Int. J. Mach. Tool Des. Res.*, 16 (1976), pp.335 - 349.
[28] Shih, A.J., Finite element analysis of orthogonal metal cutting mechanics, *Int. J. Mach. Tools Manufact.*, 36 (1996), 2, pp.255-273.
[29] Dogu, Y., Aslan, E., Camuscu, N., A numerical model to determine temperature distribution in orthogonal metal cutting, *J. Mater. Process. Technol*., 171 (2006), 1, pp.1-9.
[30] Ozel, T. *Investigation of high speed flat end milling process prediction of chip formation, cutting force, tool stresses and temperatures*, PhD dissertation, The Ohio State University, USA, (1998)
[31] Soo, S.L., Aspinwall, D.K., Dewesa, R.C., 3D FE modelling of the cutting of Inconel 718, *J. Mater. Process. Technol.*, 150 (2004), 1-2, pp.116–123.

Paper submitted: February 3, 2012
Paper revised: April 16, 2012
Paper accepted: May 2, 2012